

SHEAR-WAVE ANISOTROPY IN THE AUSTIN CHALK, TEXAS, FROM MULTIOFFSET VSP DATA: CASE STUDIES

GARETH S. YARDLEY¹ AND STUART CRAMPIN¹

ABSTRACT

The Austin Chalk is an important reservoir rock in which productivity and direction of fluid flow are predominantly controlled by the presence of fractures. Recent work has shown these fractures to be anisotropic to seismic waves. In this paper, we analyze VSP data from three sites along the Austin Chalk trend to determine the anisotropic structure of the region and investigate the link between anisotropy and reservoir productivity. The anisotropy parameters of polarization direction and time delay are extracted from the data sets using currently available anisotropy estimation techniques. Most of the observed time delay builds up in the near-surface layers, and the polarization directions of the leading split shear waves follow regional fracture and stress directions. Multioffset VSP data from the BP test site near Devine, Texas, are modelled using a combination of crack and thin-layer anisotropy to give a structure with orthorhombic symmetry which yields a good match between observed and synthetic results. Shear-wave data, also from Devine, generated by a P-wave source and by mode conversions are also analyzed and yield similar results to the direct shear-wave data. Zero-offset VSP data from Burleson and Dimmit counties, supplied by Amoco, are also examined. The Burleson VSP was acquired in a producing well. The chalk layer at this site is too thin for observable time delays to build up in transmitted shear waves, but the analysis of reflected arrivals shows a correlation between anisotropy and productivity in the Austin Chalk.

INTRODUCTION

Productivity in the Austin Chalk is controlled by the presence of fractures (Kuich, 1989). Such fractures occur in clusters and recently have been the target of horizontal drilling programs with over 80% of horizontal drilling in the United States taking place in this region (Mueller, 1992). To intersect the maximum number of fractures, horizontal wells need to be drilled perpendicular to the fracture strike (Martin, 1992). The region lacks obvious structural hydrocarbon traps and it is necessary to examine ways of locating and determining the strike of the fractures, which are known to contain hydrocarbons.

The presence of aligned fractures causes the rock mass to be effectively anisotropic to the passage of seismic waves. Shear waves in anisotropic media typically split into two phases with different velocities and nearly orthogonal polarizations. For near-vertical propagation through distributions of vertical, parallel fractures, cracks, microcracks and aligned pores, the polarization direction of the leading split shear wave gives some estimate of the strike of the fractures, and the time delay between the two arrivals gives some estimate of the crack density. Hence, it has been suggested (Crampin et al., 1989) that seismic shear-wave anisotropy may be used for characterization of fractured reservoirs. Mueller (1991, 1992) and Li et al. (1993) have analyzed reflection data from the Austin Chalk trend and correlated anisotropy (implying fractures) in the chalk layer with reservoir productivity. Mueller (1991, 1992) identified areas of the Austin Chalk showing pronounced anisotropy; these were drilled and shown to be producing fractured reservoirs.

The study area lies in an intraplate basin and the general tectonic setting and stress regime has been described by Zoback and Zoback (1991). The outcrop of the Austin Chalk is shown in Figure 1 and the chalk dips at about 2° towards the Gulf of Mexico. Extension is occurring towards the Gulf of Mexico and the maximum horizontal stress is parallel to the coast. The nature of the fracturing within the chalk has been described by Corbett et al. (1987) who analyzed data from cores and surface outcrops. Fracture orientations are parallel to the regional stress directions. Studies of shear-wave anisotropy in the region find that the polarization direction of the leading split shear wave is parallel to the stress pattern (Becker et al., 1990; Raikes, 1991; Li et al., 1993).

In this paper, we analyze vertical seismic profile (VSP) data in an attempt to understand the link between anisotropy, productivity and the presence of fractures in a reservoir. VSPs with recordings over the entire depth range down to the zone of interest allow a more controlled environment in which to study the relationship between shear-wave anisotropy and

¹Edinburgh Anisotropy Project, British Geological Survey, Murchison House, West Mains Road, Edinburgh EH9 3LA; also, Department of Geology and Geophysics, University of Edinburgh, Grant Institute, West Mains Road, Edinburgh EH9 3JW

We thank Amoco and BP for supplying the data analyzed in this paper and are grateful to S.A. Raikes (BP, Sunbury) and M.C. Mueller (Amoco, Houston) for their help in obtaining the data and for many useful comments on the work. The synthetic seismograms were calculated with the ANISEIS program of Applied Geophysical Software Inc. and Macro Ltd. This research was supported, in part, by the Sponsors of the Edinburgh Anisotropy Project and the Natural Environment Research Council and is published with the approval of the EAP Sponsors and the Director of the British Geological Survey (NERC).

rock properties than do reflection lines. It is anticipated that the knowledge gained from analyzing VSP data can be applied to the analysis of reflection data to aid exploration seismology.

The locations of the three VSP sites are shown in Figure 1. BP supplied multioffset VSP data from their test site near Devine. Amoco supplied a single nine-component zero-offset VSP data set from Dimmit county and a multioffset VSP data set from Burleson county. Multioffset data greatly reduce the nonuniqueness of models.

In this paper, the Devine test site data are processed to yield the anisotropy parameters of time delay and polarization angle and a model is produced which gives a good match between observed and modelled anisotropy parameters. Zero-offset VSP data from all three sites are then used to determine the anisotropic structure of the Austin Chalk using reflected amplitudes. The analysis reported here is a summary of a wider ranging and more detailed report by Yardley (1993). The terminology for anisotropy is that supplied by Crampin (1989).

THE BP DEVINE TEST SITE

The nine-component VSP data (Raikes, 1991) from the BP test site near Devine, modelled in this paper, were acquired in June 1989 by Downhole Seismic Services using an ARCO impulsive source (ARIS). The ARIS is a forced weight drop source whose mechanism can be tilted up to 30° from the vertical giving rise to vertically propagating shear and compressional energy. The firing mechanism is tilted to each side and fired. Each pair of shots radiates P-waves and shear waves with reverse polarities. This allows the P-wave signal to be enhanced and the shear wave cancelled by adding the

two recorded signals, whereas subtracting the signals cancels the P-wave signal and enhances the shear waves. In this operation, two shots were stacked to give the shear-wave source and four shots were stacked to give the P-wave source at each geophone level.

The acquisition geometry is shown in Figure 2. Three-component data were recorded simultaneously in all three wells from each source position in turn. The ARIS source was used to acquire P-wave data and shear-wave data with two source polarizations (in-line and cross-line) at each source position giving a total of nine nine-component VSPs.

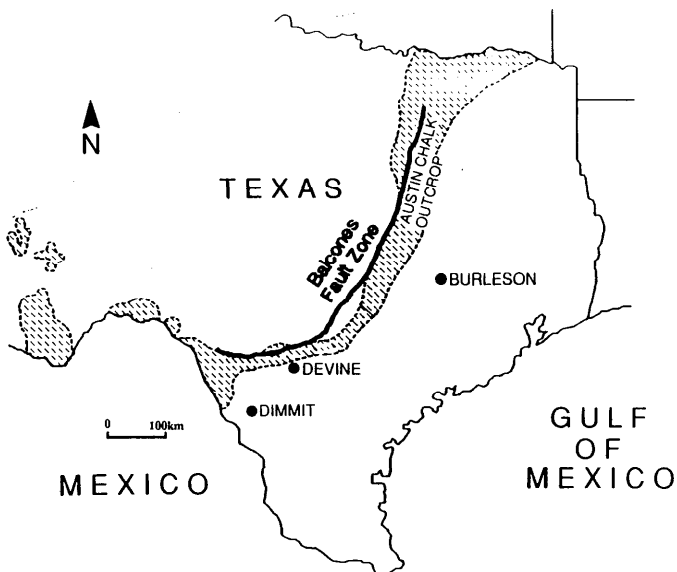


Fig. 1. Map showing the locations of the three sites analyzed in this paper. The shaded area is the Austin Chalk outcrop. Adapted from Corbett et al. (1987) and Kuich (1989).

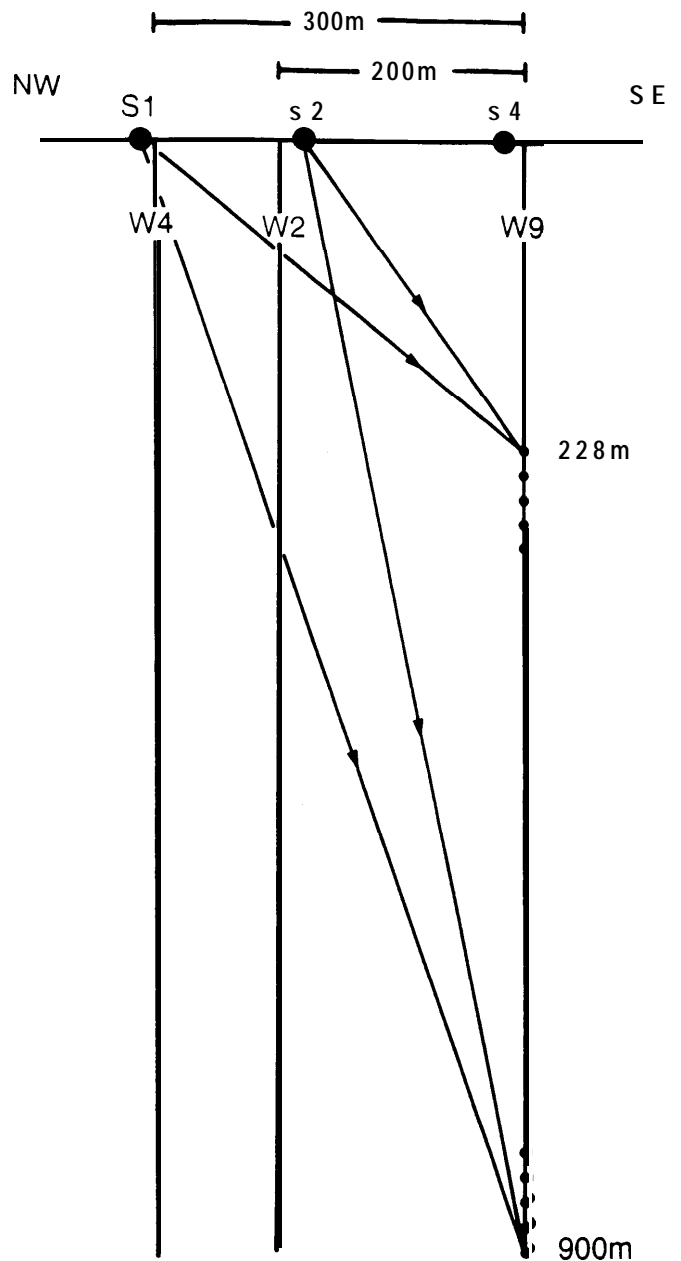


Fig. 2. Cross-section through the BP Devine test site showing the source (labelled S) and borehole (labelled W) locations used in this study. The wells and source positions lie along a single NW-SE azimuth. Geophone levels were at 8-m intervals from 228 m to 900 m with some near-surface geophone levels in the zero-offset VSPs.

To aid processing, the data were arranged by offset; the offset groupings are shown in Table 1. VSP data sets are identified by well name and source location.

Table 1. Source offsets at the BP Devine test site.

Offset grouping	VSP name	Offset
Zero-offset	W4S1	9 m
	W2S2	19 m
	W9S4	15 m
115-m offset	W2S1	110 m
	W4S2	119 m
185-m offset	W2S4	186 m
	W9S2	183 m
300-m offset	W4S4	287 m
	W9S1	311 m

The data are generally of very good quality. Figure 3 shows sample shear-wave VSPs from one of the furthest offsets (300 m). Minimal standard processing was applied to the data to avoid disturbing shear-wave signals. The data had been rotated (Raikes, 1991) into the radial and transverse coordinate system using angles determined by analysis of *P*-wave arrivals. Deconvolution was not initially applied to the data as the arrivals are generally short and the anisotropy estimation techniques use the whole arrival to calculate results meaning that it is not necessary to collapse the waveform. A quadrilateral *f-k* filter was applied to remove the upgoing wave field. Campden (1990) showed that *f-k* filters applied to three-component data sets do not distort shear-wave signals. For this data set, the filter decreases the scatter in the results of the various anisotropy estimation techniques (Yardley, 1993). Removal of the upgoing wave field is necessary before propagator matrix techniques can be applied as these assume that the recorded wave field at one level is the source for deeper levels.

EXTRACTION OF ANISOTROPY PARAMETERS FROM DEVINE VSPs

A selection of currently available anisotropy estimation techniques were used to extract the anisotropy parameters of polarization angle and time delay (Wild et al., 1993). Each of the techniques used has its own particular benefits and when used together provide a robust estimate of the anisotropy parameters. Zeng and MacBeth (1993), in this issue, give the mathematical formulations for some of these techniques and discuss their accuracy.

The dual-source cumulative technique, DCT (Zeng and MacBeth, 1992), an analytical form of the source geophone rotation (Alford, 1986), and the dual-source independent technique, DIT (MacBeth and Crampin, 1991; Zeng and MacBeth, 1992), were used on the offset data (see Wild et al., 1993). DCT is the most widely used dual-source estimation technique and determines the angle that minimizes the recorded energy on the off-diagonal elements of the four-component data matrix by effectively rotating the source and geophones. DIT is similar to DCT but the sources and geo-

phones are rotated independently. This gives two polarization angle results, one for the geophone rotation and one for the source rotation. For a constant crack strike both these results are coincident. Differences between the source and geophone results may indicate changes in crack orientation with depth, particularly for zero-offset VSPs (MacBeth and Yardley, 1992).

Estimation techniques on zero-offset data

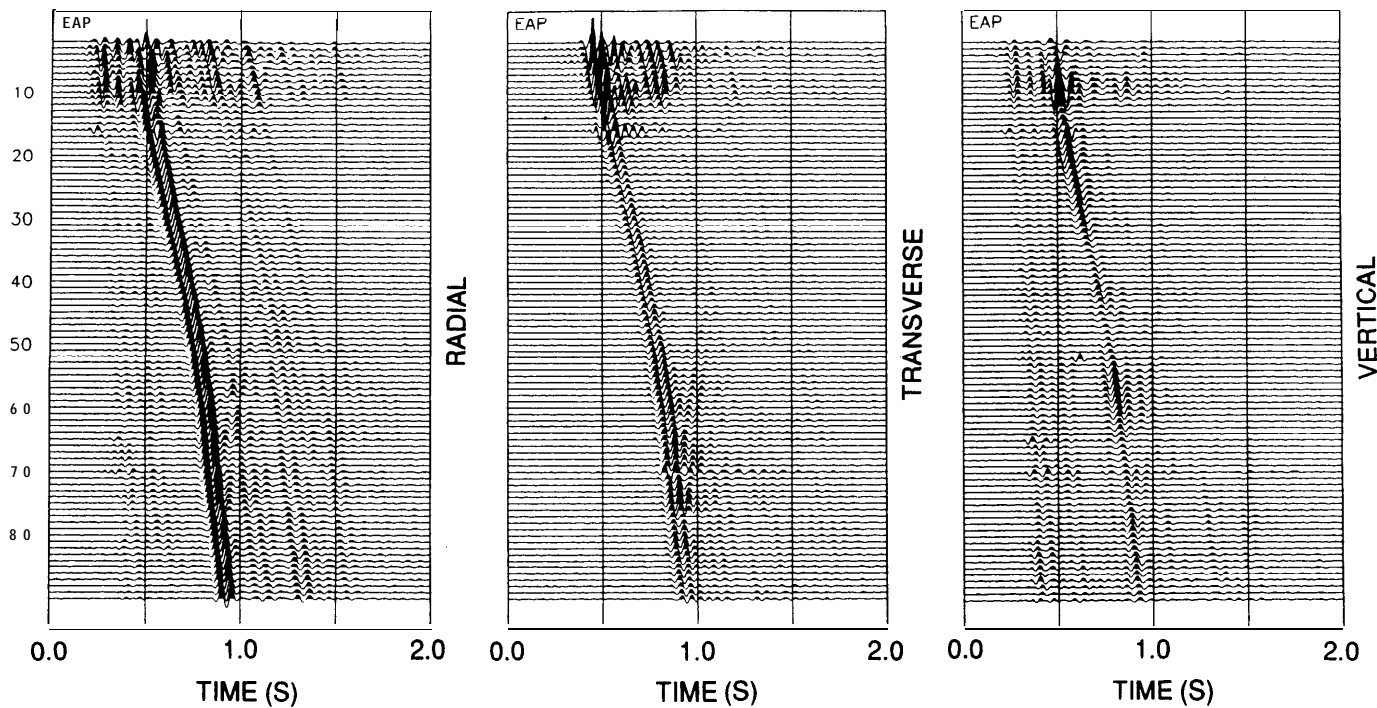
The data were collected without a gyroscope survey and the linear transform technique (Li and Crampin, 1991, 1993) was applied to the zero-offset data to determine the geophone orientation and the polarization direction of the leading split shear wave. This technique assumes that the crack strike is constant with depth. An analysis of window lengths for these calculations (Yardley, 1993) showed once the whole of the main downgoing arrival was included in the time window the results are stable. All further windows were picked using an interactive program to include the main downgoing signal. The assumption of constant crack strike seems reasonable. This region is geologically simple with subhorizontal layering and a uniform regional stress field. Reflection surveys find time delays which gradually increase with depth implying a constant crack orientation (Alford, 1986; Li et al., 1993).

Results from W2S2 are shown in Figures 5 and 6; W4S1 gave similar results. Most of the time delay builds up in the top 250 m and the total time delay at depth is 12.8 ± 1.6 ms. The polarization direction of the leading split shear wave, for W2S2, is constant around $N62.0 \pm 1.9^\circ$ E for the upper anisotropic layers. W9S4 gave similar time-delay results but gave polarization angles of $N50 \pm 5^\circ$ E. These results are consistent with dipmeter and televiewer data which show dipping fractures in W4 and W9 striking $N68^\circ$ E and $N40^\circ$ E, respectively (S.A. Raikes, pers. comm.).

Estimation techniques on offset data

For offset data most of the shear-wave energy may not be in the horizontal plane. The horizontal plane is usually used to calculate the anisotropy parameters as it provides a fixed reference frame in which to display measured polarization directions. Also, for a purely hexagonal anisotropic symmetry the two split shear waves are necessarily orthogonal, an assumption of many estimation techniques, but their projections onto a horizontal plane are not orthogonal except for incidence in the plane parallel to the crack strike. Processing techniques DCT and DIT were applied in the plane containing the shear-wave energy (the dynamic axes) and also in the horizontal plane to evaluate their effectiveness. The incidence angle of the incoming shear wave, from the in-line source, was computed as the angle orthogonal to the measured polarization of the wave in the sagittal plane. (The sagittal plane is the vertical plane containing source and geophone.) The wave polarization was determined using a 300 ms time window around the shear-wave arrival. These angles were used to rotate the data into the dynamic axes. Estimates

DEVINE: W9S1 300m Offset - Inline source



DEVINE: W9S1 300m Offset - Crossline source

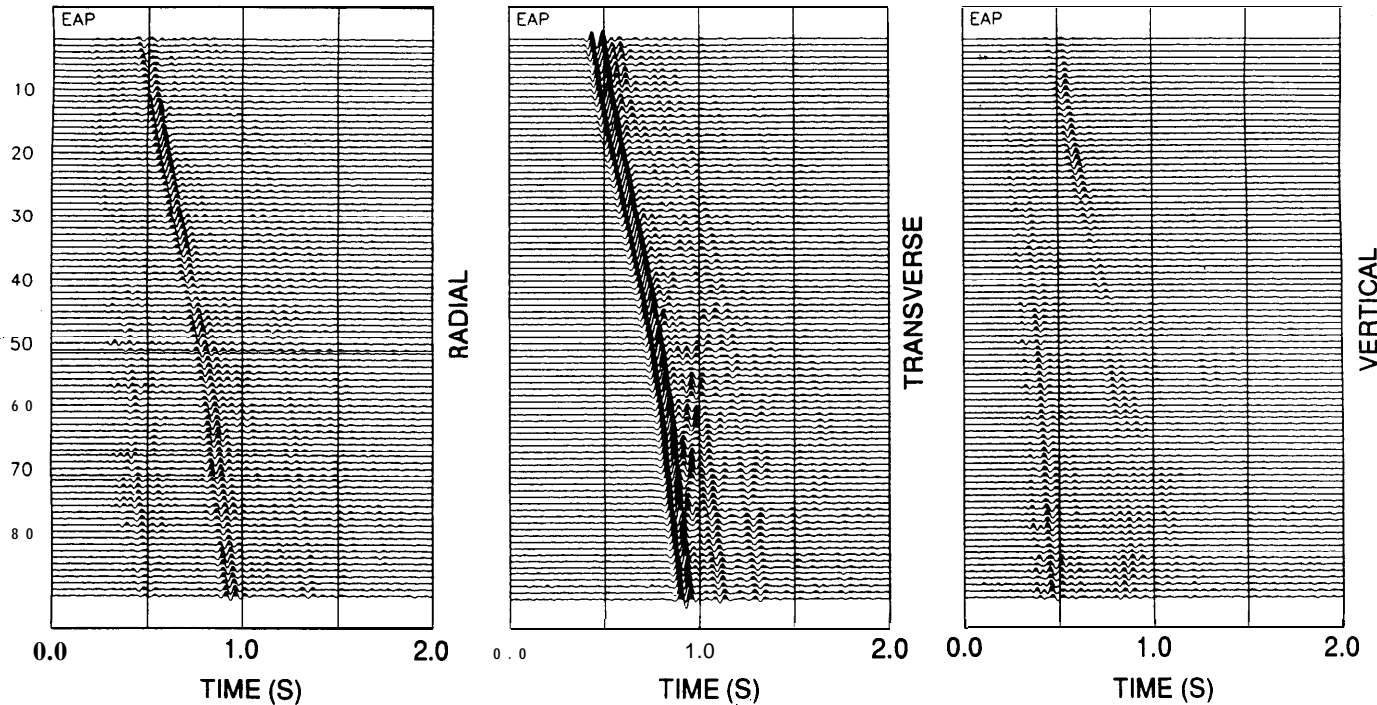


Fig. 3. Three-component seismograms from a 300-m offset VSP at Devine. At a given level the seismograms from the in-line source are scaled relative to the radial component and the transverse component for the cross-line source. A small amount of energy is present on the off-diagonal sections indicating anisotropy. For this offset there is also shear-wave energy on the vertical component as the waves are not travelling vertically.

of the polarization direction of the leading split shear wave, calculated in the dynamic coordinate system, were projected back onto a horizontal surface. This means that all displayed polarization estimates are with respect to a fixed coordinate system. Measured incidence angles in the zero-offset data were from 0° to 10° for the 115-m offset VSPs, from 0° to 20° for the 185-m offsets, and up to 85° for the near-surface geophone levels in the 300-m offset VSPs, but between 5° and 35° for geophone levels below 450 m.

There will be some errors in the calculated incidence angles, since in anisotropic media the group velocity is not perpendicular to the wavefront except in particular symmetry directions (Crampin, 1981, 1989). For the anisotropic model developed later in this paper this deviation is up to 8°. How-

ever, with incidence angles which are, in general, up to 30° the dynamic plane is preferable to the horizontal plane for estimating polarization angle and time delay as it contains more of the shear-wave energy.

In-line and cross-line sources have different shear-wave radiation patterns which means, for offset data, that the recorded signals from the in-line and cross-line sources have different energies. Versions of DCT and DIT which equalize the energy on the off-diagonal sections were used to overcome this. This source-balancing technique assumes that there is no multiple splitting. The effects of using source balancing and the dynamic plane are shown in Figure 4. The example shown is for a 300-m offset VSP as this has the largest incidence angles and the largest differences in source

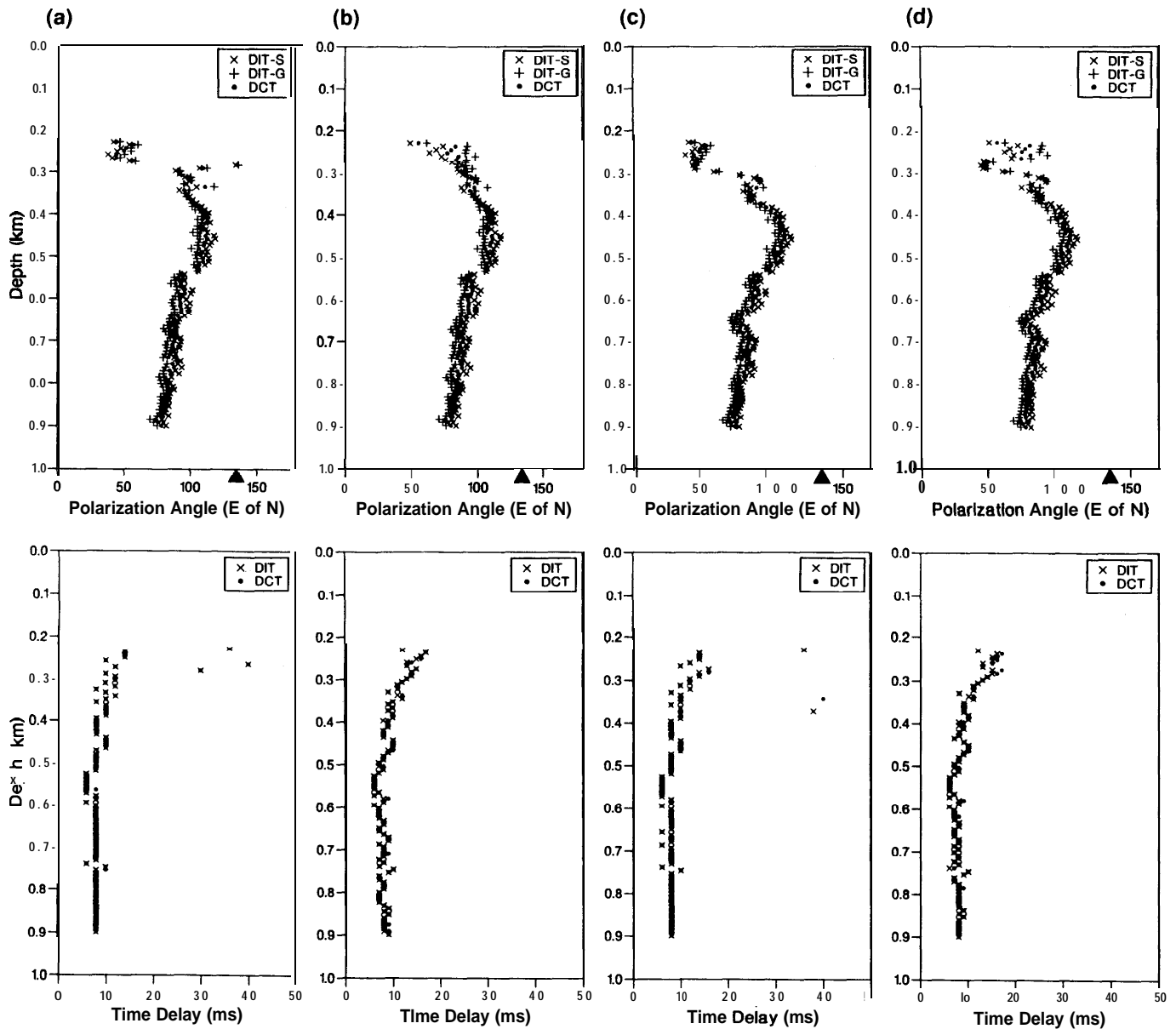


Fig. 4. A comparison of different analysis methods on data from W9S1 (300-m offset): (a) DCT and DIT applied to wave motion in the horizontal plane; (b) source-balanced versions of DCT and DIT applied to wave motion in the horizontal plane; (c) DCT and DIT applied in the dynamic plane; (d) source-balanced versions of DCT and DIT applied in the dynamic plane. The in-line direction is marked by a triangle. The sampling rate is 2 ms; however, the source-balancing version used here linearly interpolates the rotated traces to give time delay measurements in 1-ms increments.

energies. Most of the observed changes in the estimates are the effects of performing the calculations in the dynamic axes, although the changes are not great and are mostly seen in the polarization estimates. Zeng and MacBeth (1993) show that source strengths must differ by at least 50% before the estimated polarization angle changes by more than 5° from the true value. This suggests that the source-balancing correction is not generally significant. Source and geophone estimates from DIT are close to each other implying no multiple splitting (MacBeth and Yardley, 1992).

Figures 5 and 6 show the results of applying DCT in the dynamic plane for all offsets. At depth, time-delay and polarization-angle results are similar for all offsets. However, the near-surface results are offset-dependent as expected because the anisotropy parameters are dependent on azimuth and incidence angle in anisotropic media. The VSPs in each offset grouping have opposite azimuthal directions but the results of the estimation techniques are consistent for all VSPs at a given offset.

Further estimation techniques were also applied to the data. A propagator matrix technique (Zeng and MacBeth,

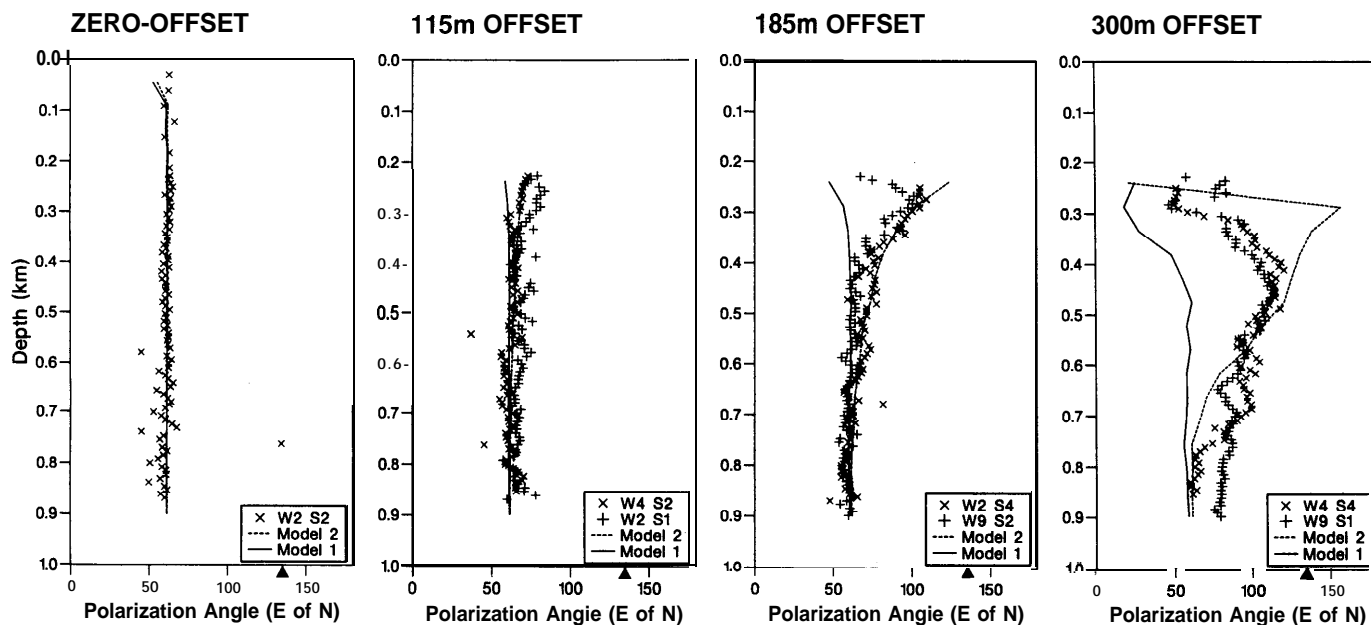


Fig. 5. A comparison of modelled and observed polarization angles at each offset for the BP test site. Estimates were calculated using the linear-transform technique on the zero-offset field data and DCT in the dynamic axes for all other data. Model 1 contains only vertical cracks; Model 2 has additional PTL anisotropy in the upper two layers (see Table 2). The in-line direction is marked by a triangle.

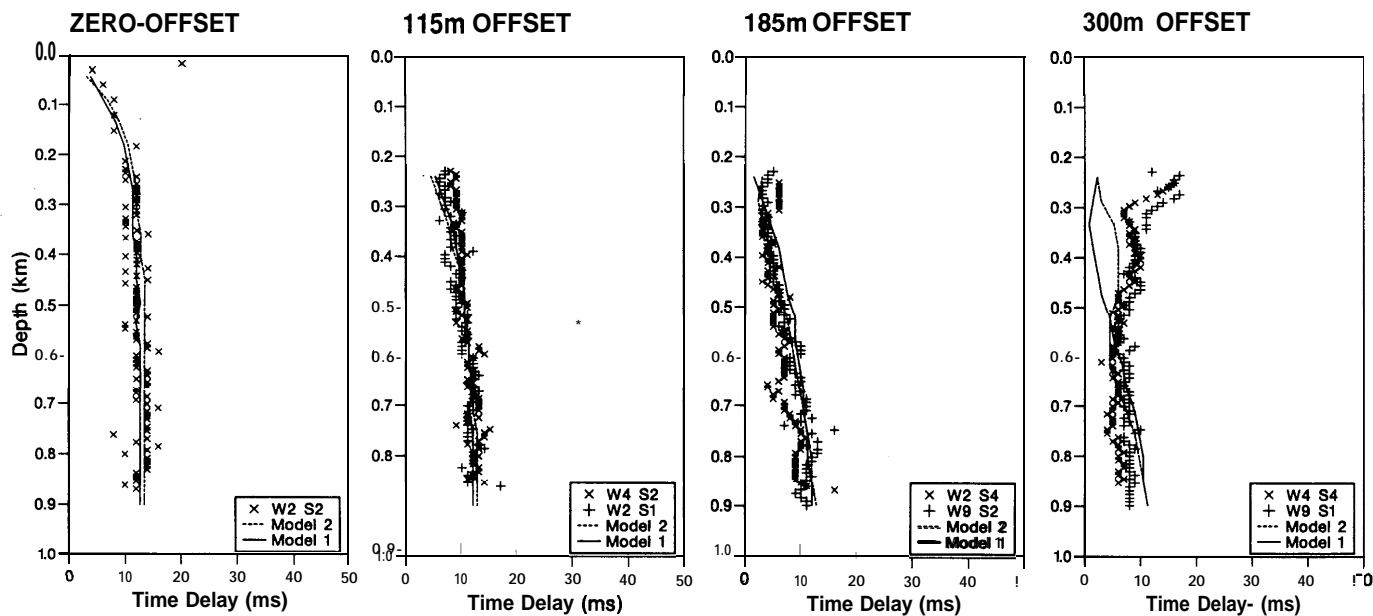


Fig. 6. A comparison of modelled and observed time delays at each offset for the same models and estimation techniques as in Figure 5 for the BP test site. The delays are the total time delay built up from source to receiver.

1992) was applied to the 115-m offset data. This technique, which requires near-offset rotated data, looks at interval measurements between geophones. The propagator matrix technique was tested on intervals of 5, 10 and 15 geophone levels and gave polarization angle estimates of $N64 \pm 15^\circ E$ (not shown). The scatter is due to errors in geophone rotation and the small increase in time delay over the region examined. However, the result confirms that there is little change in crack orientation with depth and that the observed anisotropy is real and not a product of near-surface mode conversions, which may give apparent anisotropy (Campden et al., 1990). A direct time series single-source technique (Campden, 1990) was also applied to all offset data to check that the dual-source techniques used above were correctly combining the data from the two sources. Results were scattered, as the time delay is small and the particle motions are nearly linear, but were consistent with the dual-source techniques.

Raikes (1991) obtained similar results by assuming that the polarization of the faster split shear wave, $qS1$, was either perpendicular or parallel to the in-line direction and timing the arrivals from the two sources. This suggested a $qS1$ polarization within about 10° of the cross-line direction and gave a time delay of 12 ms at depth.

Anisotropy parameters from mode-converted shear waves

Collecting shear-wave data using separate shear-wave sources is expensive. The shear-wave field in the P-wave VSP sections was examined to see if it could yield information about the anisotropy parameters consistent with the dual-source techniques. The results have implications for marine VSPs where all shear energy comes from P-to-SV mode conversions.

Examination of the offset VSP sections showed a shear-wave arrival created at or near the source, seen on both the in-line and cross-line sections, and deeper mode-converted events seen only on the in-line sections. Analyzing mode-converted shear-wave data is more difficult than analyzing data collected from a shear-wave source as only one polarization is generated and the shear energy has to be separated from strong compressional energy. The shear-wave arrival created at or near the source is spatially well separated from the compressional energy and no wave-field separation was performed. The single-source direct time series estimation technique (Campden, 1990) was applied to this arrival for all offsets (examples are shown in Figure 7). The results are similar in character to those determined above, except that the polarization estimates are rotated clockwise by 10° to 20° . It is possible that this is due to a dipping mode-converting interface which would give an initial shear-wave source polarization which was not in the in-line direction. Although the polarization direction of the leading split shear wave is determined by the medium, the estimation technique uses the source polarization as a reference direction. This means that

insufficient knowledge of the source may lead to errors in the estimated polarization directions. Some scatter is expected as the time delays are small, there is only one source polarization, and the $qS1$ polarization for the medium is almost orthogonal to the in-line direction. The deeper mode conversions were examined in a similar way, except that the estimation technique was applied in the dynamic plane to minimize interference from the compressional wave field. Polarization estimates lay along the in-line (source) direction and time-delay results were very scattered indicating little anisotropy at depth or that the rays pass near a shear-wave singularity (Crampin, 1991). From the previous work it is expected that there is little anisotropy at depth.

This has shown that P-wave sources can provide sufficient direct and mode-converted shear-wave energy to enable the anisotropic parameters to be determined, although it is preferable to optimize the acquisition geometry, by such techniques as those of MacBeth et al. (1993), so that the suspected crack strike is not parallel or perpendicular to the in-line direction and splitting can be clearly seen in the polarization diagrams.

MODELLING OBSERVATIONS AT DEVINE

Before modelling, the likely causes of the anisotropy must be investigated. The geological section is a sequence of sub-horizontal layers. In the upper structure, down to the Anacacho Limestone at 594 m (Figure 8), these are predominantly shales with interbedded limestones, sandstones and clays and thin-layer anisotropy is likely [as found by Miller et al. (1992) in the deeper shales]. The results from the estimation techniques also indicate some azimuthal anisotropy which cannot be attributed to subhorizontal layering. It is known (Corbett et al., 1987) that the Austin Chalk is fractured and these fractures are the likely cause of azimuthal anisotropy in this layer (Mueller, 1991, 1992). However, in the near-surface layers, where the rock is less consolidated, the anisotropy is probably due to aligned pores, fluid-filled microcracks and cracks known as extensive-dilatancy anisotropy, or EDA (Crampin, 1993).

As dipping fractures were found in the Austin Chalk at this site (S.A. Raikes, pers. comm.) it is possible that dipping cracks are the cause of the anisotropy in the near-surface layers (see also Crampin, 1990). However, the consistency between anisotropy parameters (Figures 5 and 6) from the two offset VSPs in each offset grouping, with opposite radial directions, implies that the structure has a horizontal plane of symmetry. A structure of dipping cracks, unless they dip in a direction 90° to the acquisition line (and the fractures found at depth do not), cannot display such bilateral symmetry. An orthorhombic system made from a combination of horizontal thin layers and vertical cracks (Wild and Crampin, 1991) is the simplest anisotropic structure consistent with the geology of the region.

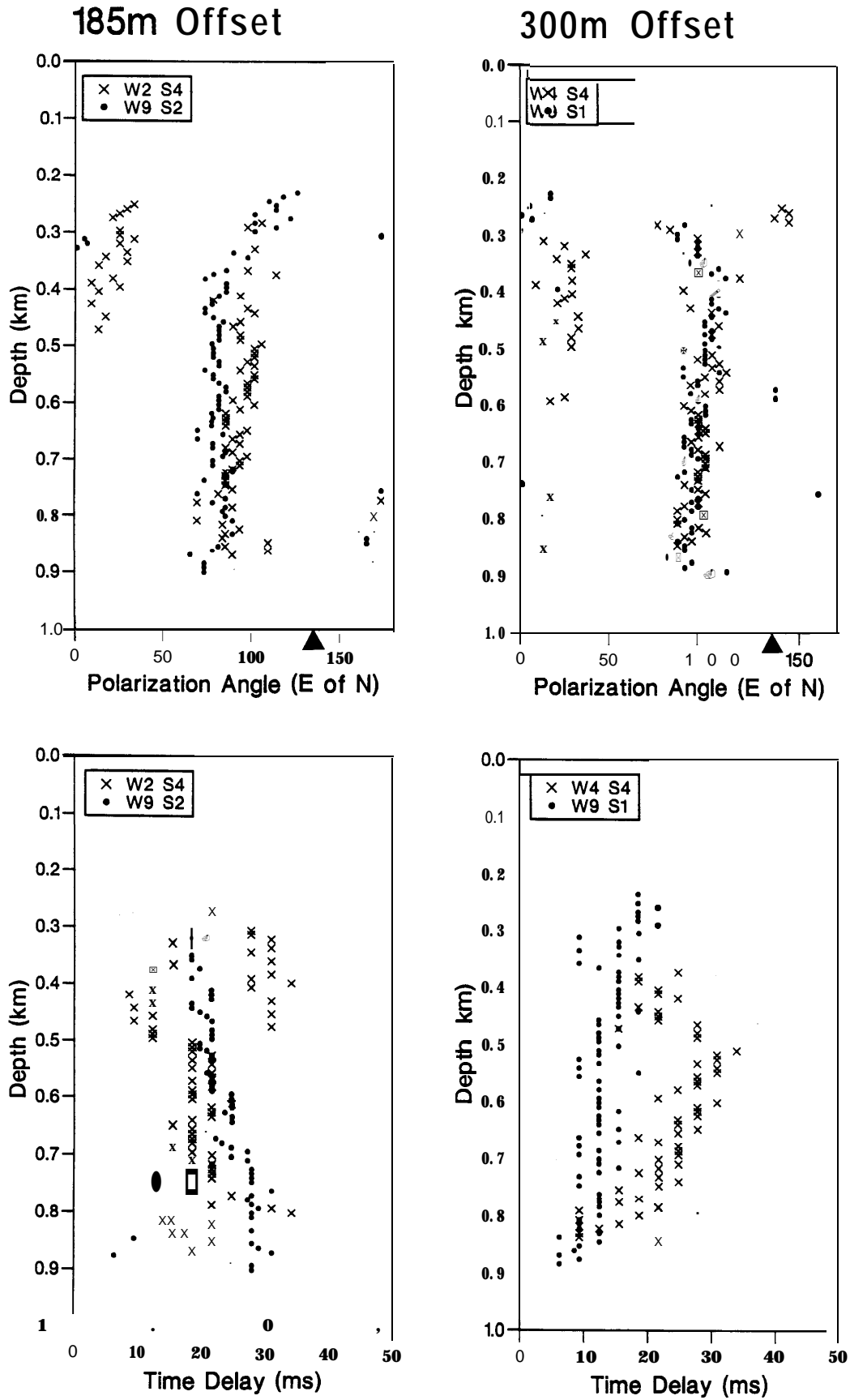


Fig. 7. Results of the single-source direct time series estimation technique (Campden, 1990) applied to the direct shear-wave arrival from the 185-m and 300-m offset P-wave sources at the BP test site. The in-line direction is marked by a triangle.

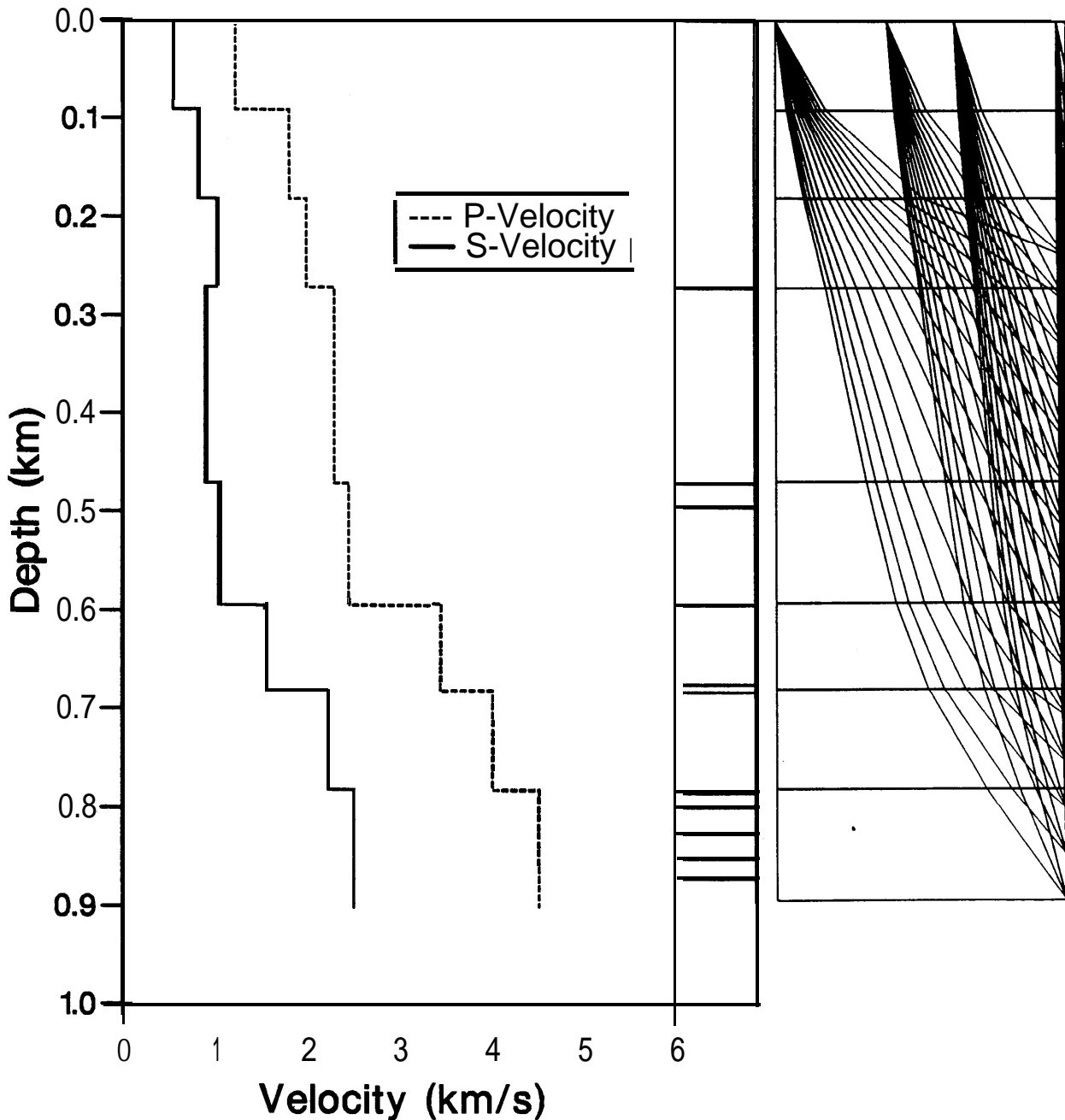


Fig. 8. Isotropic velocity structure for the BP Devine test site together with a geological section and shear-wave ray tracing through the structure. The modelling assumes that the structure is laterally invariant and that it has a horizontal axis of symmetry. Therefore, each of the real offset VSP groupings (containing either two or three VSPs) are modelled as a single VSP. These have offsets of zero (10 m), 115 m, 185 m and 300 m. The geological formations are: (a) shales with interbedded limestones; (b) shales; (c) Olmos Sand; (d) Anacacho Clay; (e) Anacacho Limestone; (f) Pecan Gap Limestone; (g) Austin Chalk; (h) Eagle Ford Shale; (i) Buda Limestone; (j) Del Rio Clay; (k) Georgetown Limestone and (l) Edwards Limestone.

Modelling anisotropic structures

The geological structure of this region of Texas consists of subhorizontal layers and it is therefore appropriate to use the ANISEIS modelling package (Taylor, 1990) which calculates full-waveform synthetic seismograms using an anisotropic version of the reflectivity technique. This package uses the formulations of Hudson (1980, 1981) [as adapted by Crampin (1984)] and Hudson (1986) to insert

penny-shaped cracks into an isotropic rock mass to simulate crack anisotropy. The crack density, ϵ , is given by $\epsilon = Na^3/V$, where N is the number of cracks of radius a in volume V ; this gives a differential shear-wave anisotropy of approximately $\epsilon \times 100\%$ for thin cracks. The thin-layer anisotropy expected from the plane-layered structure is modelled in this paper as periodic thin-layer (PTL) anisotropy made up of two alternating layers, chosen to give the required elastic properties.

The layers do not have to alternate to produce an anisotropic medium (Backus, 1962); however, some periodicity of layering is required to form uniform transversely isotropic layers. The elastic constants of the PTL material were computed using the formulations of Postma (1955). These elastic constants were then used as the matrix material into which cracks were inserted using the formulations of Hudson. In this paper, we match the polarizations and time delays measured from the field data with polarizations and time delays measured by the same techniques applied to synthetic seismograms calculated with ANISEIS. This is preferred to matching polarization diagrams in this present data set, as the time delays are small and the shear-wave particle motions are almost linear elongated ellipses with no distinctive features. Furthermore, it is not necessary to know the exact signature of the ARIS.

Isotropic model for Devine

The rock mass at Devine is laterally invariant over the 300 m between W4 and W9 (Raikes, 1991; Miller et al., 1992) and a single anisotropic model was sought to explain the results of the estimation techniques for all offsets. Therefore, only one VSP from each offset grouping is modelled. A full set of well logs was available from W9 to aid modelling.

An isotropic model was created by inverting arrival times from the $qS1$ polarization section from W2S2 using layer boundaries from well logs. The isotropic velocities gave a good match to the velocities from well logs. Ray tracing through the model is shown in Figure 8. For a medium containing thin cracks the $qS1$ velocity is the isotropic matrix velocity. The effect of cracking the medium is to slow the second arrival. V_p was calculated from the shear-wave velocity structure using V_p/V_s values from well logs. Densities were taken directly from well logs. Model parameters are shown in Table 2. The incidence angles determined from ray tracing through the isotropic model were found to be about 10° greater than those determined previously for the field data.

Anisotropic models for Devine

Full-waveform synthetic seismograms through model structures were calculated with ANISEIS and the anisotropy parameters were estimated using DCT in the dynamic plane. Zero-offset results were first modelled to match the crack structure (thin-layer anisotropy has no anisotropic effects for exactly vertical propagation). Cracks with crack densities of up to 0.038 (approximately 4% anisotropy) striking at $N62^\circ E$ were required in the upper four layers of the model to match the observed anisotropy parameters (see Table 2 and Figures 5 and 6). A similar amount of anisotropy confined to the upper structure has been found elsewhere in sedimentary basins (Bush and Crampin, 1991). Synthetic seismograms were calculated for the offset source positions and anisotropy parameters estimated. The results are shown as Model 1 in Figure 5 for polarizations and Figure 6 for time delays. The results fit well for the near offsets; however, the fit degenerates with offset and a zero time delay is seen in the 300-m

Table 2. Parameters for models of BP's Devine test site.

ISOTROPIC MODEL PARAMETERS				
Layer	Thickness (km)	Density (g/cm ³)	V_p (km/s)	V_s (km/s)
1	0.092	2.20	1.236	0.562
2	0.090	2.20	1.822	0.828
3	0.090	2.20	2.000	1.031
4	0.198	2.25	2.300	0.905
5	0.124	2.20	2.460	1.050
6	0.088	2.50	3.440	1.550
7	0.101	2.50	4.000	2.217
8	Half-space	2.50	4.500	2.488

ANISOTROPIC MODEL PARAMETERS			
	Crack strike (N $^\circ$ E)	Crack density ϵ	% PTL anisotropy
Model 1			
Layer 1	62 $^\circ$	0.038	
Layer 2	62 $^\circ$	0.026	
Layer 3	62 $^\circ$	0.013	
Layer 4	62 $^\circ$	0.007	
Model 2			
Layer 1	62 $^\circ$	0.038	4.0
Layer 2	62 $^\circ$	0.026	4.0
Layer 3	62 $^\circ$	0.013	4.0
Layer 4	62 $^\circ$	0.007	4.0

Cracks have a radius of 0.001 m, an aspect ratio of 0.01 and are water-filled.

offset modelled data, at a depth of 340 m, but not in the field observations. This behaviour is associated with the line singularity (Crampin, 1989) for a distribution of vertical cracks.

The expected thin-layer anisotropy of the rock structure was modelled by the addition of PTL anisotropy to the upper four layers (Model 2 in Figures 5 and 6). A range of PTL anisotropies was tested. The model shown has 4% PTL anisotropy. Shales with interbedded clays, sandstones and limestones are present down to nearly 600 m; however, a good match was achieved with PTL anisotropy present only in the top four layers. Adding PTL anisotropy improves the fit between observed and modelled anisotropy parameters and the zero time delay, seen in Model 1 for the 300-m offset, is no longer present. The only significant mismatches are for the shallow geophone levels in the 300-m offset VSPs. As can be seen in Figure 3, there is considerable distortion for upper geophone levels from the in-line source; this is due to mode conversions for the wide offset arrivals which interfere with the shear-wave arrivals. Further distortions are caused by effects of internal shear-wave windows (Liu and Crampin, 1990) where differences in transmission coefficients for the SV and SH components lead to distortion of a generally polarized shear wave for nonnormal incidence.

The estimation techniques were applied to the synthetic data in the dynamic plane. The incidence angles were calculated in the same way as for the field data. It was found that these incidence angles were up to 8° smaller than those determined by isotropic ray tracing and gave a better fit to the calculated incidence angles from the field data. This was

expected as the group velocity is not parallel to the wavefront in anisotropic media.

A comparison of the field and synthetic results of the estimation techniques shows that care must be taken not to interpret estimates of the polarization angle of the leading split shear wave from offset VSPs directly in terms of the strike of vertical cracks. The remaining mismatches may be due to lateral changes in crack strike as indicated by the results of the linear-transform technique in the zero-offset VSPs and borehole information.

REFLECTED AMPLITUDES FROM CHALK LAYER

Anisotropy parameters were also calculated using the linear-transform technique for the zero-offset VSPs at all three sites. Time-delay estimates from these sites are shown in Figure 9. Polarization-angle estimates of the leading split shear wave were $N23\pm 10^\circ E$ and $N105\pm 5^\circ E$ for the Dimmit and Burleson VSPs, respectively. Polarization estimates were constant with depth and are consistent with recent results from the Dimmit (Li et al., 1993) and the northern Giddings Field (Mueller, 1991, 1992). Analysis of transmitted waves does not provide enough resolution in these cases to establish whether the chalk layers are anisotropic as there are no observable increases in time delay associated with the Austin Chalk layer. Knowing the uncertainty in the estimated time delays and the velocity in the chalk, from inversion of

first arrivals, it is possible to put upper limits on the shear-wave anisotropy. These limits are: 2%, 4% and 15% for the Dimmit, Devine and Burleson wells, respectively. The Burleson VSP was acquired in a producing well, where the chalk layer is thin and it is not possible to determine its anisotropic structure using transmitted shear waves. Field studies show that thin layers are more likely to be heavily fractured (Barthelemy et al., 1992). The study of reflected arrivals may provide the best way of studying anisotropy in thin layers (Thorsen, 1988; Yardley et al., 1991; Mueller, 1991, 1992). Here, reflected amplitudes in the zero-offset VSP data are analyzed to see if they can give a more accurate determination of the anisotropy in the Austin Chalk.

If a layer is anisotropic due to the presence of aligned vertical cracks or fractures, the shear-wave velocity will be different for waves polarized parallel and perpendicular to the crack strike. Consequently, reflection coefficients will be different for waves polarized parallel and perpendicular to the crack strike. Mueller (1991, 1992) used this effect to locate areas of high fracture intensity in the Austin Chalk. The difference in reflection coefficients for shear waves polarized parallel and perpendicular to the fractures is dependent on the percentage anisotropy and on the velocity contrast across the reflecting interface (Yardley et al., 1991; Li and Crampin, 1992).

The linear-transform technique was used to determine the $qS1$ polarization in the VSPs at all sites and the data were

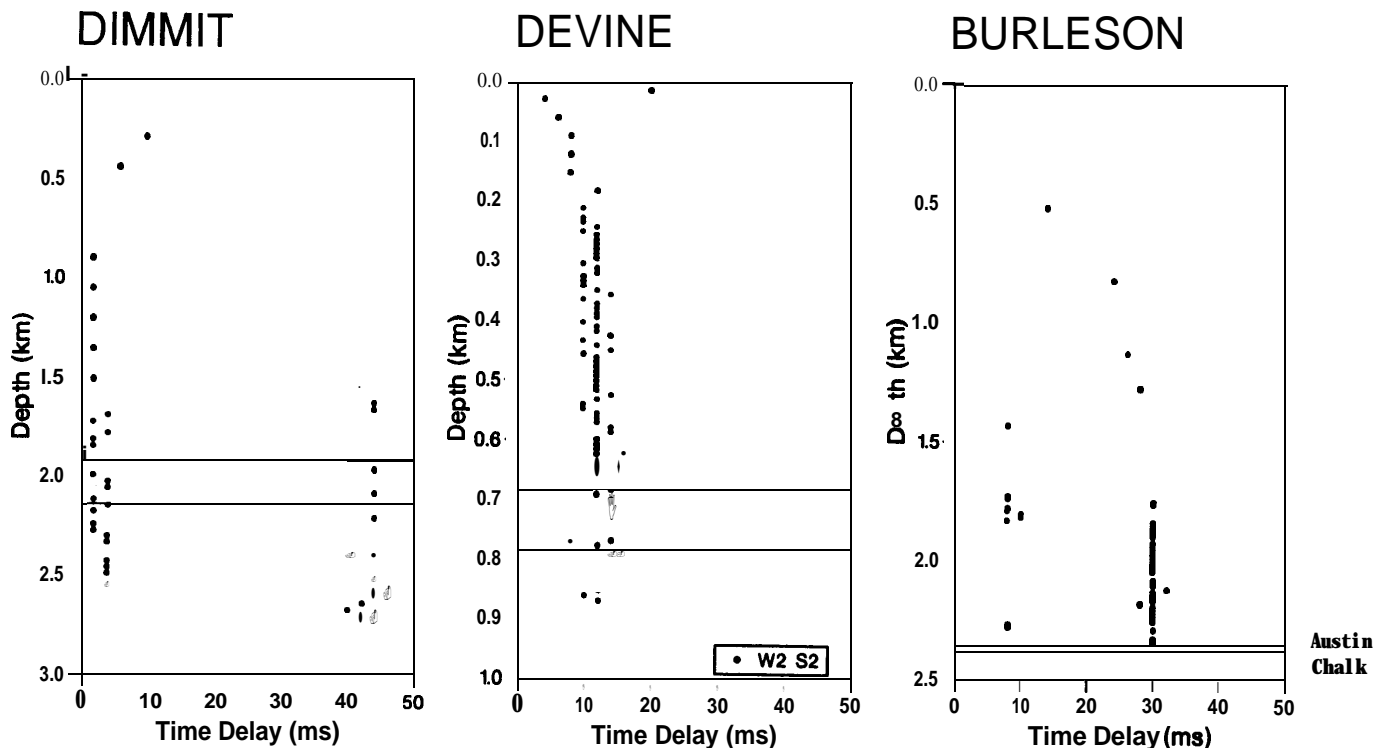


Fig. 9. Comparison of zero-offset time delays estimated from field data at the three study sites. The spurious results around 44 ms in the Dimmit VSP and 8 ms in the Burleson VSP are due to cycle skipping in the crosscorrelation to determine time delay. The high time-delay values for the shallow geophone levels in the Dimmit VSP are due to a 13-m difference in the in-line and cross-line source positions leading to an apparent time delay between arrivals from each source.

then rotated to give the $qS1$ (parallel to the cracks) and $qS2$ (perpendicular to the cracks) sections. The data were normalized and the upgoing and downgoing wave fields separated using quadrilateral $f-k$ filters. Before the amplitude ratio of the upgoing arrivals on the $qS1$ and $qS2$ sections could be calculated the upgoing event was normalized with respect to the downgoing arrival at each geophone level. This means that changes in source strength between the in-line and cross-line sources and spherical divergence effects can be neglected. The amplitude ratio was then calculated at each level for a given reflector. The reflection from the Austin Chalk is generally weak and deconvolution operators were designed using the whole wave field to compress the arrival (Smidt, 1989). Amplitude ratios were calculated for all limestone and chalk reflectors at the three sites, before and after wave-field compression. Example results for reflections from the Austin Chalk layer after wave-field compression are shown in Figure 10. In cases where the in-line direction was almost perpendicular to the $qS1$ polarization (Dimmit and Devine) the $qS1$ section was calculated from the cross-line source energy and the $qS2$ section from the in-line source to improve the signal-to-noise ratio. At Burleson the $qS1$ direction was between the in-line and cross-line directions and enough energy was present on the in-line and cross-line geophone components to calculate amplitude ratios for each source orientation.

Correlation of anisotropy with production

The Burleson VSP is the only one of the three data sets to be collected in a producing well. As the hydrocarbon reservoirs in the Austin Chalk are fractured, it is expected that these reservoirs are anisotropic to shear-wave propagation and it may be possible to identify fractured chalk from analysis of the reflected amplitude ratios. Figure 10 shows that the average amplitude ratios for the chalk reflectors for the Dimmit VSP and for W4S1 at Devine are close to unity indicating that the chalk layer is effectively isotropic as expected from the analysis of transmitted waves. W2S2 (100 m from W4S1) has scattered results. Scatter in the results is due to inadequate estimation of the $qS1$ polarization and interference between reflected arrivals from different levels. Standard deviations were calculated to show the uncertainty in the calculated amplitude ratio.

The amplitude ratios at Burleson are less than unity suggesting an anisotropic chalk layer. This cannot be stated with absolute certainty as the amplitude ratio lies within one standard deviation of unity. The effect on the amplitude ratio of a thin anisotropic layer is likely to be small. It would be necessary to conduct high-frequency experiments to be able to say for certain that the chalk layer is anisotropic. However, the analysis of reflected amplitudes may be the only method available to examine anisotropy in thin layers where insufficient time delays build up for transmitted wave analysis.

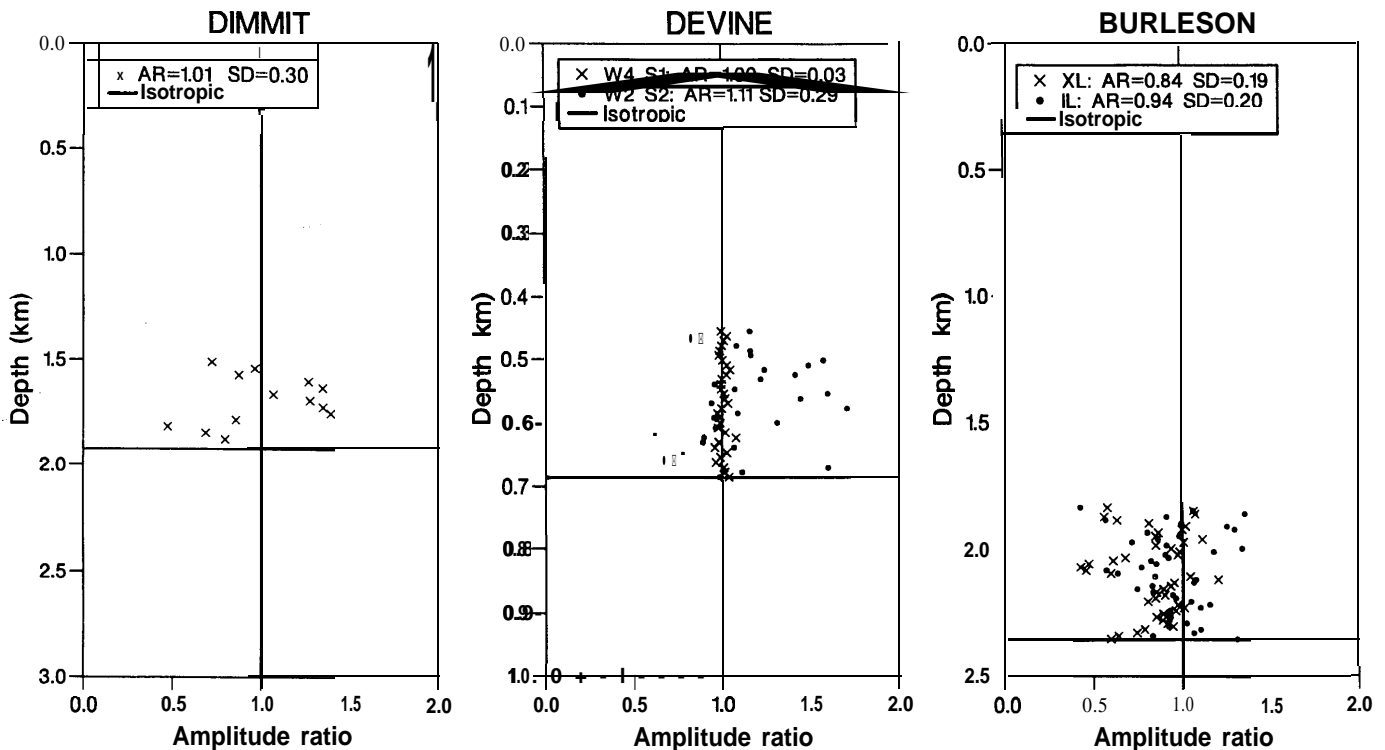


Fig. 10. Comparison of amplitude ratios calculated at each geophone level at the three field sites. Averaged amplitude ratio (AR) and standard deviation (SD) for the reflectors are given in the legends. The amplitude ratios are scattered, because of the weak reflectors, and cluster around a value of 1.0 as expected for isotropic reflectors. At Burleson the in-line (IL) and cross-line (XL) data give amplitude ratios below unity implying an anisotropic reflector.

Modelling of horizontally layered structures (Yardley, 1993) shows that even for thin layers, where the upgoing event is a superposition of reflections from the top and bottom of the layer, any deviation in amplitude ratio from unity indicates an anisotropic reflecting layer. [The situation is more complex if the reflectors dip as reflection coefficients also vary with incidence angle (Achenbach, 1973).] The analysis of the reflected amplitudes at the three VSP sites indicates that only the Burleson well penetrates an anisotropic chalk layer. Without detailed knowledge of the velocity structure and pulse shape it is not possible to quantify the amount of anisotropy in the reflecting layer, but for these sites it is found that there is a positive correlation between anisotropy and productivity in the chalk layer.

CONCLUSIONS

This paper has raised a number of points concerning the processing, modelling and interpretation of shear-wave data in the presence of anisotropy. These points are summarized below.

1. Using dynamic axes to calculate the anisotropy parameters for offset data allows more of the shear-wave energy to be used in the calculation. This leads to different estimates of the polarization angle than those obtained by performing the calculation in the horizontal plane. Balancing the energy from in-line and cross-line source orientations in offset VSPs does not produce significant changes in the results of anisotropy estimation techniques.
2. In this region of Texas, most of the observed time delay is built up in the near-surface. The polarization direction of the faster split shear wave is constant with depth and is parallel to the regional stress and fracture patterns in this tectonically simple area.
3. A good match can be achieved between the results of the anisotropy estimation techniques on field and synthetic seismograms using a model with orthorhombic symmetry. This anisotropic symmetry is due to a combination of horizontal thin layering (PTL anisotropy) and vertical cracks (EDA cracks), whose strike is consistent with the strike of known fractures in the wells.
4. Reflected amplitudes, whilst not being able to quantify the level of anisotropy, can be used to show whether a layer is anisotropic even if that layer is thin. The use of reflected amplitudes in locating areas of high fracture intensity can be readily adapted for use in shear-wave exploration using reflection data (Mueller, 1991, 1992). Reflected amplitudes may provide the only way to investigate reservoir anisotropy for thin layers where insufficient time delays build up to use transmitted waves.
5. For the three VSP sites examined in this paper there is a positive correlation between productivity and anisotropy in the Austin Chalk layer. This analysis has shown that the study of shear-wave anisotropy can give the information about fracture intensity and orientation necessary for exploitation of reservoirs in the Austin Chalk.

REFERENCES

- Achenbach, J.D., 1973, Wave propagation in elastic solids: North Holland Publ. Co.
- Alford, R.M., 1986, Shear data in the presence of azimuthal anisotropy: Dilley, Texas: 56th Ann. Internat. Mtg., Soc. Expl. Geophys., Exp. Abstr., 476-479.
- Backus, G.E., 1962, Long-wave elastic anisotropy produced by horizontal layering: *J. Geophys. Res.* **67**, 4427-4440.
- Barthelemy, P., Tremolieres, P. and Andrieux, J., 1992, Fracture spacing related to bed thickness: geological or mechanical bed limits?: 4th Eur. Assn. Petr. Geol. Conf., Abstr., 156-157.
- Becker, D.F., Bishop, G.W., Clayton, K.N., Peterson, D.N., Rendleman, C.A. and Shah, P.M., 1990, Shear-wave anisotropy at Marcelina Creek: at the Vector Wave Field Seismology Update Workshop, Soc. Expl. Geophys., San Francisco, Abstr.
- Bush, I. and Crampin, S., 1991, Paris Basin VSPs: case history establishing combinations of fine-layer (or lithologic) anisotropy and crack anisotropy from modelling shear wavefields near point singularities: *Geophys. J. Internat.* **107**, 433-447.
- Campden, D.A., 1990, Analysis of multicomponent VSP data for shear-wave anisotropy: Ph.D. thesis, Univ. of Edinburgh.
- _____, Crampin, S., Majer, E.L. and McEvelly, T.V., 1990, Modelling the Geysers VSP: a progress report: *The Leading Edge* **9**, 8, 36-39.
- Corbett, K., Friedman, F. and Spang, J., 1987, Fracture development and mechanical stratigraphy of Austin Chalk, Texas: *Bull. Am. Assn. Petr. Geol.* **71**, 17-28.
- Crampin, S., 1981, A review of wave motion in anisotropic and cracked elastic-media: *Wave Motion* **3**, 343-391.
- _____, 1984, Effective anisotropic elastic-constants for wave propagation through cracked solids: *Geophys. J. Roy. Astr. Soc.* **76**, 135-145.
- _____, 1989, Suggestions for a consistent terminology for seismic anisotropy: *Geophys. Prosp.* **37**, 753-770.
- _____, 1990, Alignment of the near-surface inclusions and appropriate crack geometries for geothermal hot-dry-rock experiments: *Geophys. Prosp.* **38**, 621-631.
- _____, 1991, Effects of point singularities on shear-wave propagation in sedimentary basins: *Geophys. J. Internat.* **107**, 531-543.
- _____, 1993, Arguments for EDA: *Can. J. Expl. Geophys.* **29**, 18-30.
- _____, Lynn, H.B. and Booth, D.C., 1989, Shear-wave VSPs: a powerful new tool for fracture and reservoir description: *J. Petr. Tech.* **5**, 283-288.
- Hudson, J.A., 1980, Overall properties of a cracked solid: *Math. Proc. Camb. Phil. Soc.* **88**, 371-384.
- _____, 1981, Wave speeds and attenuation of elastic waves in material containing cracks: *Geophys. J. Roy. Astr. Soc.* **64**, 133-150.
- _____, 1986, A higher order approximation to the wave propagation constants for a cracked solid: *Geophys. J. Roy. Astr. Soc.* **87**, 265-274.
- Kuich, N., 1989, Seismic fracture identification and horizontal drilling: keys to optimizing productivity in a fractured reservoir, Giddings Field, Texas: *Gulf Coast Assn. Geol. Soc., Trans.* **39**, 153-158.
- Li, X.-Y. and Crampin, S., 1991, Linear-transform technique for analyzing shear-wave splitting in four-component seismic data: 61st Ann. Internat. Mtg., Soc. Expl. Geophys., Exp. Abstr., 476-479.
- _____, and _____, 1992, Variation of reflection coefficients with crack strike and density in anisotropic media: 54th Mtg., Eur. Assn. Expl. Geophys., Exp. Abstr., 86-87.
- _____, and _____, 1993, Linear-transform techniques for processing shear-wave anisotropy in four-component seismic data: *Geophysics* **58**, in press.
- _____, Mueller, M.C. and Crampin, S., 1993, Case studies of shear-wave splitting in reflection surveys in South Texas: *Can. J. Expl. Geophys.* **29**, 189-215.
- Liu, E. and Crampin, S., 1990, Effects of the internal shear-wave window: comparison with anisotropy induced splitting: *J. Geophys. Res.* **95**, 11,275-11,281.
- MacBeth, C. and Crampin, S., 1991, Processing of seismic data in the presence of anisotropy: *Geophysics* **56**, 1320-1330.
- _____, and Yardley, G.S., 1992, Optimal estimation of crack strike: *Geophys. Prosp.* **40**, 849-872.
- _____, Wild, P., Crampin, S. and Brodov, L.Y., 1993, Optimal acquisition geometry for determining seismic anisotropy: *Can. J. Expl. Geophys.* **29**, 132-139.

- Martin, R.B., 1992, Horizontal drilling: making your well a success: The Leading Edge **11**, 8, 21-28.
- Miller, D.E., Costa, J. and Schoenberg, M., 1992, Inversion for the Devine anisotropic structure: 54th Mtg., Eur. Assn. Expl. Geophys., Exp. Abstr., 88-89.
- Mueller, M.C., 1991, Prediction of lateral variability in fracture intensity using multicomponent shear-wave surface seismic as a precursor to horizontal drilling in the Austin Chalk: Geophys. J. Internat. **107**, 409-415.
- _____, 1992, Using shear waves to predict lateral variability in vertical fracture intensity: The Leading Edge **11**, 2, 29-35.
- Postma, G.W., 1955, Wave propagation in a stratified medium: Geophysics **20**, 780-806.
- Raikes, S.A., 1991, Shear-wave characterization of BP Devine test site, Texas: 61st Ann. Internat. Mtg., Soc. Expl. Geophys., Exp. Abstr., 65-68.
- Smidt, J.M., 1989, VSP processing with full downgoing-wavefield deconvolution applied to the total wavefield: First Break **7**, 6, 247-257.
- Taylor, D.B., 1990, ANISEIS manual, version 4.5: Applied Geophysical Software Inc., Houston.
- Thomsen, L., 1988, Reflection seismology over azimuthally anisotropic media: Geophysics **53**, 304-313.
- Wild, P. and Crampin, S., 1991, The range of effects of azimuthal isotropy and EDA anisotropy in sedimentary basins: Geophys. J. Internat. **107**, 513-529.
- _____, MacBeth, C., Crampin, S., Li, X.-Y. and Yardley, G.S., 1993, Processing and interpreting vector wave-field data: Can. J. Expl. Geophys. **29**, 117-124.
- Yardley, G.S., 1993, Processing and modelling of shear-wave VSPs in anisotropic structures: case studies: Ph.D. thesis, Univ. of Edinburgh.
- _____, Graham, G. and Crampin, S., 1991, Viability of shear-wave amplitude versus offset studies in anisotropic media: Geophys. J. Internat. **107**, 493-503.
- Zeng, X. and MacBeth, C., 1992, Algebraic processing techniques for estimating shear-wave splitting: 54th Mtg., Eur. Assn. Expl. Geophys. Exp. Abstr., 622-623.
- _____, and _____, 1993, Accuracy of shear-wave polarization estimates from near-offset VSP data: Can. J. Expl. Geophys. **29**, 246-265.
- Zoback, M.D. and Zoback, M.L., 1991, Tectonic stress field of North America and relative plate motions, in Slemmons, D.B., Engdahl, E.R., Zoback, M.D. and Blackwell, D.D., Eds., Neotectonics of North America: Geol. Soc. Am.